Proceedings of 12th Cambridge Workshop on Cool Stars, Stellar Systems, & The Sun, 2003 University of Colorado.

Tracing the Spot Evolution on the Moderately-Rotating K1-Giant σ Geminorum

K. G. Strassmeier

Astrophysical Institute Potsdam (AIP), Germany

Zs. Kővári

Konkoly Observatory, Budapest, Hungary

A. Washuettl, M. Weber

Astrophysical Institute Potsdam (AIP), Germany

J. B. Rice

Brandon University, Canada

J. Bartus

Konkoly Observatory, Budapest, Hungary

Abstract. We present a simultaneous photometric and spectroscopic imaging analysis of the long-period RS CVn binary σ Gem, covering 3.6 consecutive rotation cycles with high time resolution. From six overlapping but consecutive Doppler maps we trace the evolution of individual spots throughout the time range covered. All spots group either along a band at approximately $+45°$ latitude and a width of $30°$, or appear centered at the equator. No polar spot is detected. We did not find a conclusive migration pattern from the cross-correlation maps from one rotation to the next and attribute this to a masking effect of short-term spot changes.

1. Doppler Images for 1996/97

σ Geminorum is a member of the long-period RS CVn-type binary group. The K1 giant primary component rotates with $P_{\rm rot} \approx 20$ days and shows all signs of solar-like magnetic activity. The astrophysical data for the star are summarized in Table 1 (Kővári et al. 2001).

Between 1/11/1996 and 9/01/1997 we took 52 high resolution optical spectra during the 3.6 rotation cycle- (70 days) long observing run at National Solar Observatory with the McMath-Pierce telescope. Our aim is to describe the time evolution of the surface temperature distribution during the 70-day long spectroscopic coverage. From the 52 spectra, we prepared six data subsets (SS1-SS6) in a way that each subset covers one rotation period and the successive subsets

(SSi and SS$i+1$) overlap each other by half of a rotation. Thus, subsets SS1, SS3 and SS5, as well as SS2, SS4 and SS6, represent contiguous stellar rotations without overlapping. The time evolution of the surface temperature distribution is investigated by applying our line profile inversion code TempMap to each of the six data subsets. For our Doppler analysis in this poster we use the Fe I 6430 Å line rather than the neighbouring Ca I line at 6439 Å because the iron line has a smaller equivalent width, and thus provides more surface resolution than the Ca line (for the comparison of the Fe and Ca maps see the upcoming paper by Kővári et al. 2001). The Doppler images for the Fe I 6430 Å line is presented in Fig. 1 .

Table 1 : Astrophysical data for σ Gem.

Parameter	Value
Classification	K1 III
Distance (Hipparcos)	37.5±1.1 pc
Luminosity, L	$52.5^{+14.5}_{-8.2}$ $L_\odot$
$\log g$	$2.5^{+0.23}_{-0.42}$
$T_{\rm eff}$	4630±100 K
$(B-V)_{\rm Hipparcos}$	1.118±0.006 mag
$(V-I)_{\rm Hipparcos}$	1.12±0.05 mag
$v \sin i$	27.5±1 km s^{-1}
Inclination, i	60°±15°
Period, $P_{\rm rot} = P_{\rm orb}$	19.60447±0.00007 days
Orbital eccentricity, e	0.0
Radius, R	$12.3^{+1.6}_{-1.0} R_\odot$
Microturbulence for Fe, $\xi_{\rm Fe}$	1.0 km s^{-1}
Macroturbulence, $\zeta_{\rm R} = \zeta_{\rm T}$	3.0 km s^{-1}
Chemical abundances	solar (adopted)

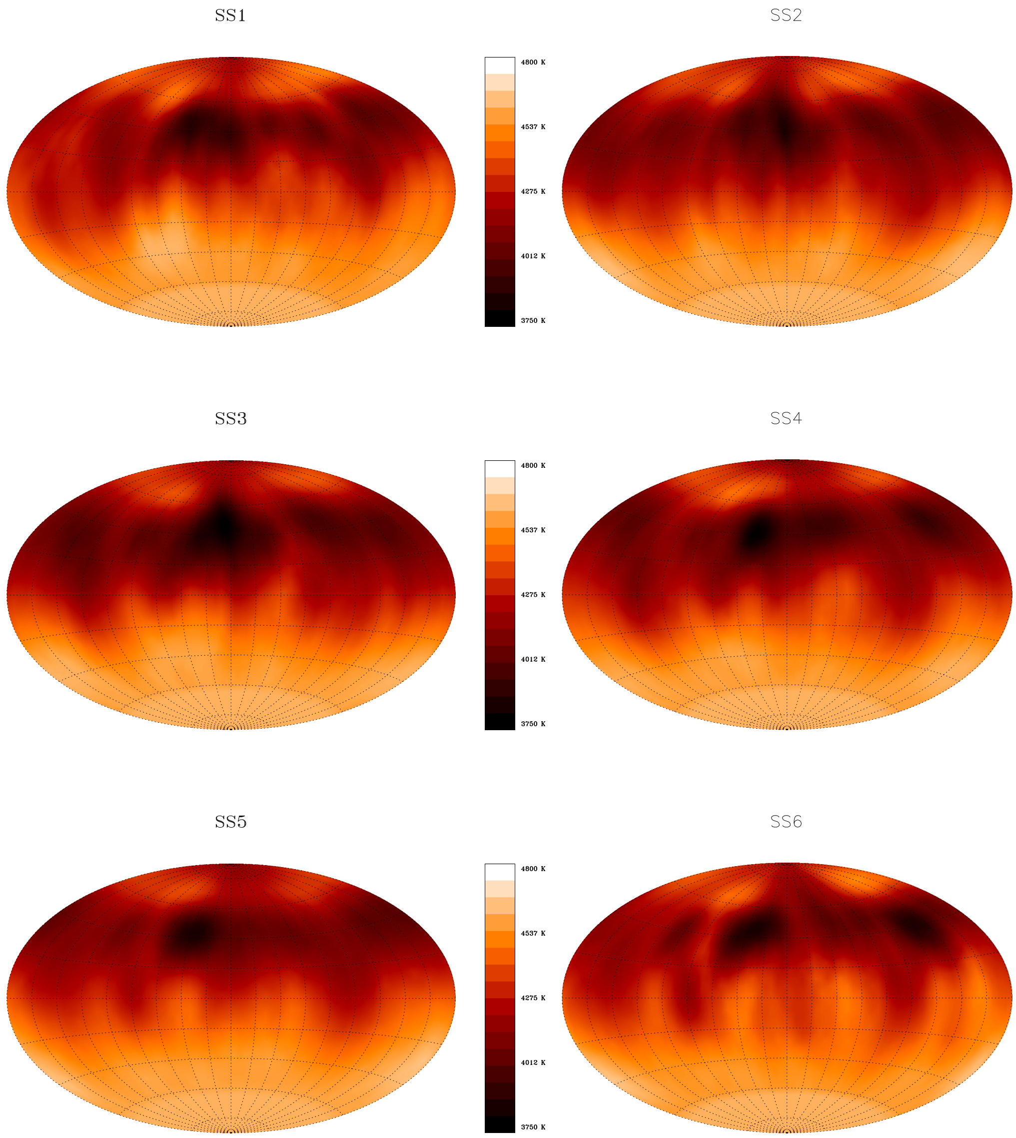

Fig. 1 : Fe I 6430 Å Doppler images of σ Gem for six epochs covering 3.6 rotation cycles.

2. Short-term Spot Evolution

To trace the different surface structures, we firstly identify individual spots on each map. Up to eleven features are may be identified and are marked with capital letters A to K in Fig. 2 . Some of them are suspiciously weak and we would normally not regard them as significant, but because they are repeatedly reconstructed from the consecutive non-overlapping maps, we consider them as possibly real. If so, we may use the spot position and the temperature to trace their geometrical and morphological evolution from one map to the next. The spots do not follow a simple migration pattern for every single case. Spot merging and splitting complicates the description. Sometimes it is even ambiguous to differentiate between spot migration and spot disappearance and reappearance nearby.

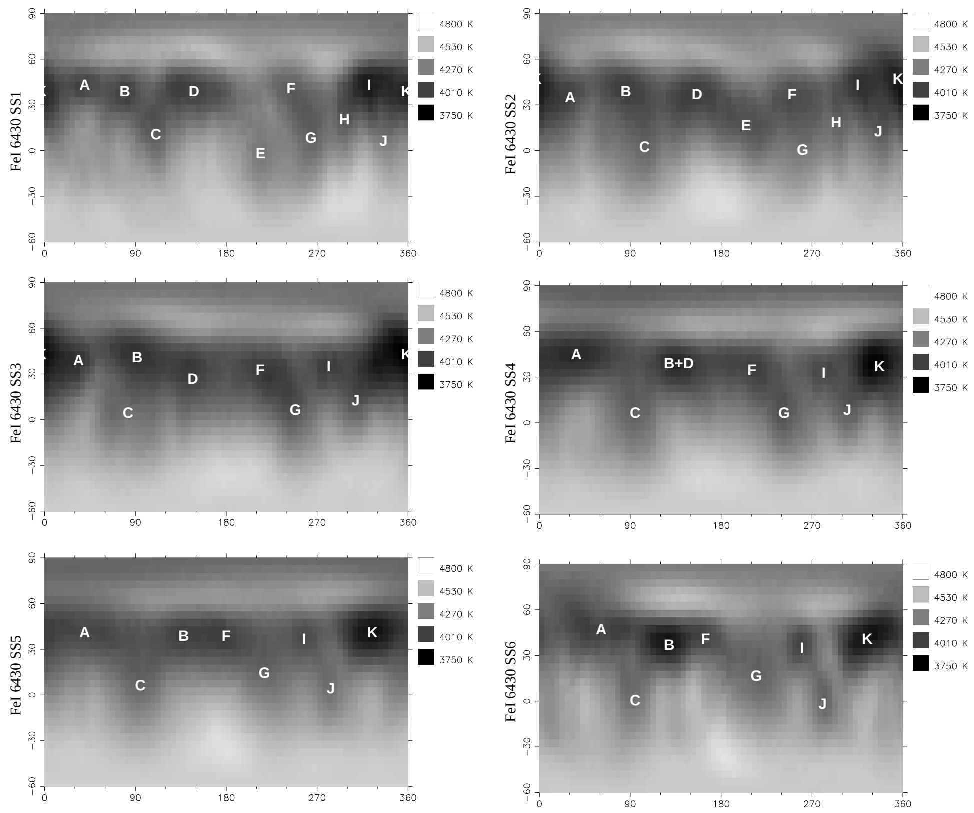

Fig. 2 : Tracing the spot evolution from the time-series Fe I-6430 Doppler images. The individual spots referred later in Fig. 3 and Table 2 are marked by capitals.

In Fig. 3 we plot the central coordinates of each spot at the mid-epochs of SS1 through SS6. The longitudinal migration distribution in the figure suggests a general migration towards smaller longitudes, i.e. falling behind the synchronuous rotational value. Some spots show a brief phase of migration towards increasing longitudes, e.g. spot B, and may be explained by a local rearrangement due to, e.g., magnetic reconnection. Table 2 summarizes the spot migrations. The average migration rate is -0.60 ± 0.82(rms) °/day with peak values of +1.23 for spot B and –1.84 for spot F.

Fig. 3b shows the central spot latitudes versus time. Spots preferably group along the equator and at a latitude of +40°. We note that the information below a latitude of approximately –30°is not well determined, even at the high S/N ratio of our data, and we cannot make a conclusive statement about the hemispheric latitudinal symmetry of the spot distribution. Spots at higher latitudes tend to move towards the visible pole with an average latitudinal migration rate of $+0.02\pm0.11$(rms)$^\circ$/day (Table 2). On the contrary, spots close to or even on the equator follow a more complicated and possibly mixed migration pattern. The average migration rates are not significant enough to interpret them in detail but it seems that the physical cause is not simply a solar-like differential rotation law but rather a complex scheme also including, e.g., diffusion by small and large scale convective motions, magnetic reconnection and meridional flows (as on the Sun). Similar phenomena were suggested – and partially observed – for the many spots on the K1-subgiant component of HR 1099 (Strassmeier & Bartus 2000).

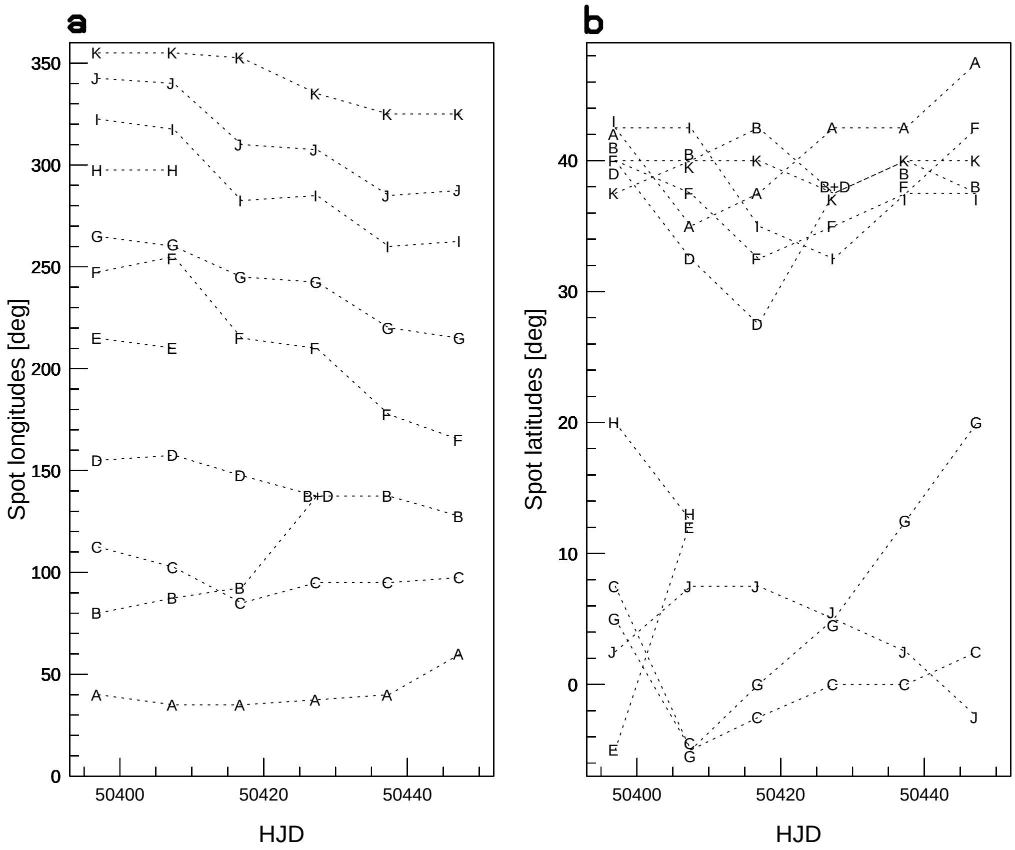

Fig. 3 : **a** Longitudinal and **b** latitudinal spot migrations during the $\approx$ 70 days long observing sequence SS1–SS6. Plotted are the central coordinates of the individual spots as indicated in Fig. 2 .

Table 2 : Spot migration rates in longitude and latitude

Spot	Longitude (deg/day)	Latitude (deg/day)
A	–0.33	+0.15
B[1]	+1.23	...
C	–0.25	...
D[1]	–0.62	...
E[2]	–0.48	...
F	–1.84	+0.04
G	–1.06	...
H[2]	0.0	...
I	–1.33	–0.12
J	–1.25	...
K	–0.73	+0.02
Average	–0.60	+0.02
rms	±0.82	±0.11

[1]omitted from the average because of strong crosstalk
[2]spot H and E appeared only during the first rotation

3. Differential Rotation?

Cross-correlation of consecutive Doppler maps is a tool to obtain a quantitative description of the surface migration pattern. Thus we cross-correlated the contiguous images, i.e. Corr{SS1/SS3}, Corr{SS2/SS4}, Corr{SS3/SS5}, and Corr{SS4/SS6} (see Fig. 4). It appears that there are two zones above and below the equator that show acceleration with respect to the synchronized rotation period while the polar regions likely lag behind. Unfortunately, we must consider this as a too weak a detection. Obviously, a simple interpretation with a latitude-dependent surface differential rotation pattern is not straightforward from our data. We believe our analysis is hampered by two facts. Firstly, the spot pattern may not have changed enough during the time of our observations in order to resolve a coherent differential-rotation signature and, secondly, the cross correlations may have been masked by individual spot evolution as shown in Fig. 2 and Fig. 3 .

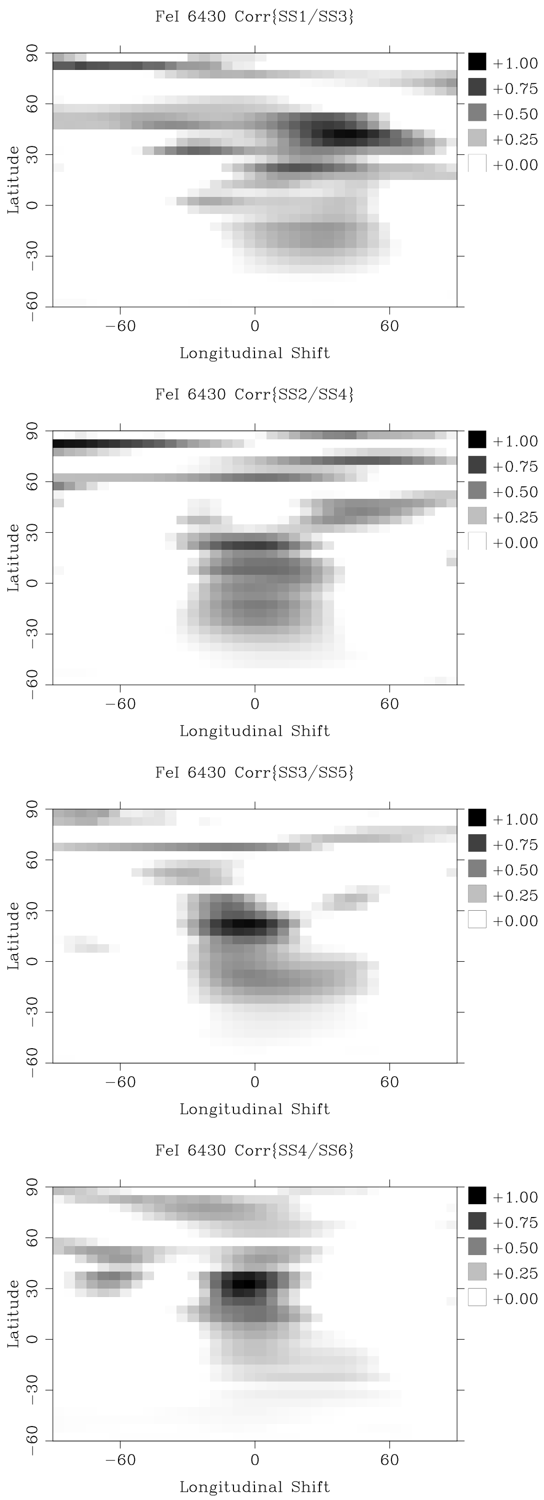

Fig. 4 : The differential migration pattern. The gray scale indicates the degree of correlation from zero (no correlation) to unity (identical).

Acknowledgments. I am grateful to the German Science Foundation for supporting our work with grants STR645/1 and HU532/8. Further information is available from the Stellar-Activity homepage at the Astrophysical Institut Potsdam. This includes a preprint server and a summary of existing Doppler images as well as tutorial pages.

References

Strassmeier, K.G., Bartus, J. 2000, A&A 354, 537

Kővári, Zs., Strassmeier, K.G., Bartus, J. Washuettl, A., Weber, M., Rice, J.B. 2001, A&A 373, 199